

Palladium–Platinum Heterobimetallic Complexes with Bridging Silicon Ligands. Structure and Reaction with Isonitrile to Afford a Platinacyclopentane Containing Si, N, and C Atoms

Tetsuyuki Yamada,[†] Makoto Tanabe,[†] Kohtaro Osakada,^{*,†} and Yong-Joo Kim[‡]

Chemical Resources Laboratory, Tokyo Institute of Technology, 4259 Nagatsuta, Midori-ku, Yokohama 226-8503, Japan, and Department of Chemistry, Kangnung National University, Kangnung 210-702, Korea

Received February 26, 2004

The reaction of $\text{Pt}(\text{SiHPh}_2)_2(\text{PEt}_3)_2$ with $\text{Pd}(\text{PEt}_3)_3$ produced heterodinuclear complexes with bridging diphenylsilyl ligands $(\text{Et}_3\text{P})\text{Pt}(\mu\text{-}\eta^2\text{-SiHPh}_2)_2\text{Pd}(\text{PEt}_3)$ (**1**) and $(\text{Et}_3\text{P})_2\text{Pt}(\mu\text{-}\eta^2\text{-SiHPh}_2)_2\text{Pd}(\text{PEt}_3)$ (**2**). Each product was isolated and fully characterized. X-ray crystallography of **2** and NMR spectra of **2** and **2-d**₂ at 25 °C indicated the presence of two bridging SiHPh_2 (or SiDPh_2) ligands, which were bonded to one metal center via a M–Si single bond and to the other via a Si–H–M three-center, two-electron bond. The ¹H NMR spectrum of **2** at –90 °C exhibited a peak at δ –8.61 due to a hydrido ligand bonded to the Pt center, indicating the structure $(\text{Et}_3\text{P})_2\text{PtH}(\mu\text{-SiPh}_2)(\mu\text{-}\eta^2\text{-SiHPh}_2)\text{Pd}(\text{PEt}_3)$ in the solution at low temperature. Complex **2** reacted with CN-*t*-Bu to form a mixture of $(\text{Et}_3\text{P})(\text{t-BuNC})\text{-Pt}(\text{SiPh}_2\text{-CH}_2\text{-N}(\text{t-Bu})\text{-SiPh}_2)$ (**3**) and $[(\text{Et}_3\text{P})(\text{t-BuNC})\text{Pt}(\mu\text{-SiPh}_2)]_2$ (**4**). Complex **3** contained the platinacyclopentane group, whose five-membered ring was composed of Pt, Si, N, and C atoms.

Introduction

Isonitrile ($\text{R-N}\equiv\text{C}$) plays an important role in organometallic chemistry not only as a ligand for transition metal complexes but also as a substrate for reactions that involve single or multiple 1,1-insertion of isonitrile into the metal–carbon bond to give the complexes with a M–C(=NR)–C group.¹ Many silyl complexes of transition metals undergo facile 1,2-insertion of C=C and C≡C bonds into the M–Si bond to form new M–C and C–Si bonds.² The number of papers on the insertion reactions of isonitriles with transition metal silyl complexes, however, is much smaller than those of the reactions of isonitriles with alkyl transition metal complexes. Silyl complexes of Sc and Zr undergo insertion of isonitrile into a M–Si bond and form complexes with η^2 -coordinated iminoacyl ligands.³ $\text{Pd}(\text{OAc})_2$ catalyzes bisilylation of aryl isonitrile with disilanes, which involves insertion of the isonitrile into the Pd–Si bonds as a crucial step.⁴ The reaction of isonitriles with Pt-

$(\text{SiHPh}_2)_2(\text{PMe}_3)_2$ was reported to cause ligand substitution, giving $\text{Pt}(\text{SiHPh}_2)_2(\text{PMe}_3)(\text{CNR})$, rather than insertion of the isonitrile into the Pt–Si bond.⁵ These results suggest that 1,1-insertion of isonitrile into Pd–Si bonds takes place more easily than that into Pt–Si bonds.

Recently we prepared a Pd–Pt heterobimetallic complex whose metal centers were bridged by two -SiHPh_2 ligands.^{6,7} Reaction of isonitriles with these heterobimetallic complexes would be of significant interest because the Pd–Si and Pt–Si bonds in the same molecule have different reactivity toward isonitrile. In this paper, we report the preparation and structures of Pd–Pt heterobimetallic complexes with PEt_3 and bridging diphenylsilyl ligands as well as the reaction of a Pd–Pt complex with an isonitrile to form a new platinacyclopentane containing Si, Pt, C, and N atoms in the five-membered ring.

[†] Tokyo Institute of Technology.

[‡] Kangnung National University.

(1) (a) Yamamoto, Y.; Yamazaki, H. *Coord. Chem. Rev.* **1972**, *8*, 225. (b) Treichel, P. M. *Adv. Organomet. Chem.* **1973**, *11*, 21. (c) Singleton, E.; Oosthuizen H. E. *Adv. Organomet. Chem.* **1983**, *22*, 209. (d) Takei, F.; Yanai, K.; Onitsuka, K.; Takahashi, S. *Angew. Chem., Int. Ed. Engl.* **1996**, *35*, 1554.

(2) (a) Tilley, T. D. In *The Silicon-Heteroatom Bond*; Patai, S., Rappoport, Z., Eds.; John Wiley & Sons: New York, 1998; Vol. 2, Part 2, Chapter 29. (b) Braunstein, P.; Knorr, M. *J. Organomet. Chem.* **1995**, *500*, 21. (c) Corey, J. C.; Braddock-Wilking, J. *Chem. Rev.* **1999**, *99*, 175.

(3) (a) Campion, B. K.; Falk, J.; Tilley, T. D. *J. Am. Chem. Soc.* **1987**, *109*, 2049. (b) Campion, B. K.; Heyn, R. H.; Tilley, T. D. *J. Am. Chem. Soc.* **1990**, *112*, 2011. (c) Campion, B. K.; Heyn, R. H.; Tilley, T. D. *Organometallics* **1993**, *12*, 2584.

(4) Ito, Y.; Sugimoto, M.; Matsuura, T.; Murakami, M. *J. Am. Chem. Soc.* **1991**, *113*, 8899.

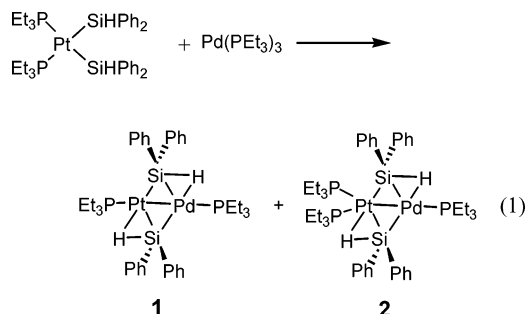
(5) Kim, Y.-J.; Choi, E.-H.; Lee, S. W. *Organometallics* **2003**, *22*, 3316.

(6) Tanabe, M.; Yamada, T.; Osakada, K. *Organometallics* **2003**, *22*, 2190.

(7) Other heterobimetallic complexes with bridging Si ligands: (a) Powell, J.; Swayer, J. F.; Shiralian, M. *Organometallics* **1989**, *8*, 577. (b) Braunstein, P.; Knorr, M.; Villarroja, E.; DeCian, A.; Fischer, J. *Organometallics* **1991**, *10*, 3714. (c) Bodensieck, U.; Braunstein, P.; Deck, W.; Faure, T.; Knorr, M.; Stern, C. *Angew. Chem., Int. Ed. Engl.* **1994**, *33*, 2440. (d) Knorr, M.; Braunstein, P.; Tiripicchio, A.; Ugozzoli, F. *Organometallics* **1995**, *14*, 4910. (e) Braunstein, P.; Morise, X. *Organometallics* **1998**, *17*, 540. (f) Braunstein, P.; Faure, T.; Knorr, M. *Organometallics* **1999**, *18*, 1791. (g) Sakaba, H.; Ishida, K.; Horino, H. *Chem. Lett.* **1998**, 149. (h) Tanabe, M.; Osakada, K. *Chem. Lett.* **2001**, 962. (i) Tanabe, M.; Osakada, K. *Inorg. Chim. Acta* **2003**, *350*, 201.

Results and Discussion

The reaction of $\text{Pt}(\text{SiHPh}_2)_2(\text{PEt}_3)_2$ with $\text{Pd}(\text{PEt}_3)_3$ produces a mixture of Pd–Pt bimetallic complexes $(\text{Et}_3\text{P})\text{Pt}(\mu\text{-}\eta^2\text{-SiHPh}_2)_2\text{Pd}(\text{PEt}_3)$ (**1**) and $(\text{Et}_3\text{P})_2\text{Pt}(\mu\text{-}\eta^2\text{-SiHPh}_2)_2\text{Pd}(\text{PEt}_3)$ (**2**) with two bridging Si-containing ligands (eq 1). Complexes **1** and **2** are isolated from the



mixture in 34% and 25% yields, respectively. There have been a number of Pt–Pt and Pd–Pd dinuclear complexes with bridging Si ligands reported so far.^{8–15} They are complexes with structures similar to **1**, $[(\text{R}_3\text{P})\text{Pt}(\mu\text{-}\eta^2\text{-SiHR}'_2)]_2$,^{8,9d} $[(\text{R}_3\text{P})\text{Pt}(\mu\text{-}\eta^2\text{-SiH}_2\text{R}')_2]$,^{13a,b,d} and $[(\text{R}_3\text{P})\text{Pd}(\mu\text{-}\eta^2\text{-SiHR}'_2)]_2$.¹⁵ The Pd complex with one phosphine ligand at one metal center and two phosphine ligands at the other, $(\text{Me}_3\text{P})_2\text{Pd}(\mu\text{-}\eta^2\text{-SiHPh}_2)_2\text{Pd}(\text{PMe}_3)$, was also prepared and characterized.¹⁵

Complex **1** was characterized by X-ray crystallography and NMR spectroscopy. Figure 1 shows the molecular structure containing a planar PdPtSi_2 four-membered ring. A crystallographic C_2 symmetry center at the midpoint of the ring imposes disorder of the positions of Pd and Pt, similarly to $(\text{Cy}_3\text{P})\text{Pt}(\mu\text{-}\eta^2\text{-SiHPh}_2)_2\text{Pd}(\text{PCy}_3)$.⁶ Thus, the molecular structure is expressed as an average of the molecules with different orientation in the crystal lattice. The distances of the two crystallographically independent metal–Si bonds differ significantly from each other (2.316(1) and 2.388(1) Å). These bonds are assigned to metal–Si single bonds and the bond in the M–H–Si group with a three-center, two-electron bond, respectively, although the hydrogen atoms were not found in the final D-map.

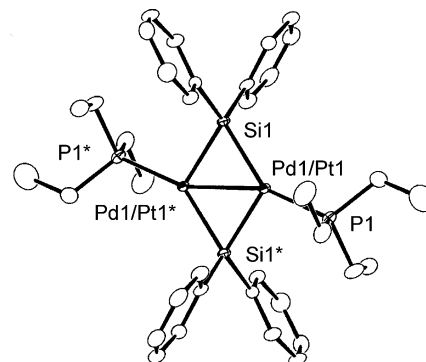


Figure 1. ORTEP drawing of **1** at the 50% ellipsoidal level. The molecule has a point of C_2 crystallographic symmetry at the midpoint of the Pd and Pt atoms. The atoms with asterisks are crystallographically equivalent to those with the same number without asterisk. Selected bond distances (Å) and angles (deg): Pd1/Pt1–Pd1*/Pt1* 2.6697(8), Pd1/Pt1–Si1 2.316(1), Pd1/Pt1–Si1* 2.388(1), Pd1/Pt1–P1 2.2889(11), P1–Pd1/Pt1–Si1 102.16(4).

The NMR data of **1** at room temperature indicate the heterodinuclear structure with M–H–Si three-center, two-electron bonds. The ^1H NMR signals for the PCH_2 hydrogens are observed as two apparent quintets due to virtual coupling at δ 1.49 and 1.27 in equal intensity. The ^1H NMR spectrum (25 °C, C_6D_6) shows doublet signals at δ 2.71 and 2.06. The ^1H – ^{195}Pt coupling constants obtained from these signals (96 and 650 Hz) indicate that the signals are attributed to Pd–H–Si and Pt–H–Si, respectively. The ^2H NMR spectrum of the complex $(\text{Et}_3\text{P})\text{Pt}(\mu\text{-}\eta^2\text{-SiDPh}_2)_2\text{Pd}(\text{PEt}_3)$ (**1-d**), obtained from the reaction of D_2SiPh_2 , contains signals at δ 2.74 and 2.07 with reasonable coupling constants ($^2J(\text{PtD}) = 15$ Hz, $^1J(\text{PtD}) = 90$ Hz). The $^{31}\text{P}\{^1\text{H}\}$ NMR spectrum exhibits two doublets at δ 28.3 and 15.8 ($^3J(\text{PP}) = 55$ Hz). The former signal, showing a much larger Pt–P coupling constant (3556 Hz) than the latter (258 Hz), is assigned to PEt_3 bonded to Pt. The ^1H and $^{31}\text{P}\{^1\text{H}\}$ NMR spectra do not change in the temperature range from –90 to 25 °C. The virtual coupling observed in the PCH_2 signals in the ^1H NMR spectrum, a large P–P coupling constant, and crystallographic results showing the metal–metal distance of 2.6697(8) Å indicate the presence of a Pd–Pt bond in the molecule.

Figure 2 shows crystallographic results of complex **2**. The Pd, Pt, and two Si atoms form a planar four-membered ring similar to **1** and other dipalladium and dipalladium complexes with two bridging silyl ligands. The phosphorus atoms of two PEt_3 ligands bonded to the Pt center are out of the plane formed by the metals and Si atoms (Figure 2b). The Pd–Pt distance (2.757(1) Å) is longer than that of **1** and is within the range of normal metal–metal bonding.¹⁶ One of the two Pd–Si bonds (2.388(3) Å) is longer than the other (2.300(3) Å), while the Pt–Si bond lengths differ by 0.06 Å (Pt–Si = 2.415(3) and 2.361(3) Å). The bond parameters suggest a structure containing Si–H–Pd and Si–H–Pt three-center, two-electron bonds (Chart 1 A), similar to $[(\text{Cy}_3\text{P})\text{Pd}(\mu\text{-}\eta^2\text{-SiHPh}_2)]_2$ (Pd–Si = 2.326(2) and 2.384(2) Å).⁶ The hydrogen positions of **2** were not found by crystallography. Braddock-Wilking obtained a dinuclear

(8) Auburn, M.; Ciriano, M.; Howard, J. A. K.; Murray, M.; Pugh, N. J.; Spencer, J. L.; Stone, F. G. A.; Woodward, P. *J. Chem. Soc., Dalton Trans.* **1980**, 659.

(9) (a) Zarate, E. A.; Tessier-Youngs, C. A.; Youngs, W. J. *J. Am. Chem. Soc.* **1988**, *110*, 4068. (b) Zarate, E. A.; Tessier-Youngs, C. A.; Youngs, W. J. *J. Chem. Soc., Chem. Commun.* **1989**, 577. (c) Anderson, A. B.; Shiller, P.; Zarate, E. A.; Tessier-Youngs, C. A.; Youngs, W. J. *Organometallics* **1989**, *8*, 2320. (d) Sanow, L. M.; Chai, M.; McConville, D. B.; Galat, K. J.; Simons, R. S.; Rinaldi, P. L.; Youngs, W. J.; Tessier, C. A. *Organometallics* **2000**, *19*, 192.

(10) Michalczyk, M. J.; Recatto, C. A.; Calabrese, J. C.; Fink, M. J. *J. Am. Chem. Soc.* **1992**, *114*, 7955.

(11) Heyn, R. H.; Tilley, T. D. *J. Am. Chem. Soc.* **1992**, *114*, 1917.

(12) Shimada, S.; Tanaka, M.; Honda, K. *J. Am. Chem. Soc.* **1995**, *117*, 8289.

(13) (a) Levchinsky, Y.; Rath, N. P.; Braddock-Wilking, J. *Organometallics* **1999**, *18*, 2583. (b) Braddock-Wilking, J.; Levchinsky, Y.; Rath, N. P. *Organometallics* **2000**, *19*, 5500. (c) Braddock-Wilking, J.; Levchinsky, Y.; Rath, N. P. *Organometallics* **2001**, *20*, 474. (d) Braddock-Wilking, J.; Levchinsky, Y.; Rath, N. P. *Inorg. Chim. Acta* **2002**, *330*, 82.

(14) Fürstner, A.; Krause, H.; Lehmann, C. W. *Chem. Commun.* **2001**, 2372.

(15) (a) Kim, Y.-J.; Lee, S.-C.; Park, J.-I.; Osakada, K.; Choi, J.-C.; Yamamoto, T. *Organometallics* **1998**, *17*, 4929. (b) Kim, Y.-J.; Lee, S.-C.; Park, J.-I.; Osakada, K.; Choi, J.-C.; Yamamoto, T. *J. Chem. Soc., Dalton Trans.* **2000**, 417.

(16) Cotton, F. A.; Walton, R. A. *Multiple Bonds between Metal Atoms*; Wiley: New York, 1982.

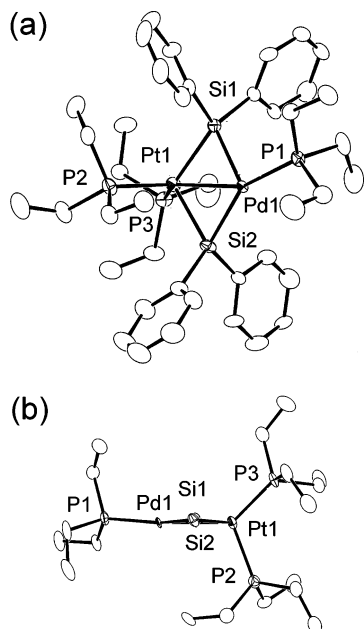
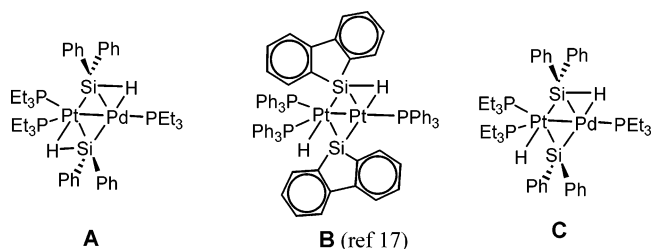


Figure 2. ORTEP drawing of **2** at the 50% ellipsoidal level. One of the two crystallographically independent molecules is shown. Selected bond distances (Å) and angles (deg): Pd1–Pt1 2.757(1), Pd1–Si1 2.300(3), Pd1–Si2 2.388 (3), Pt1–Si1 2.415(3), Pt1–Si2 2.361(3), Pd1–P1 2.281 (3), Pt1–P2 2.383(3), Pt1–P3 2.325(3), Pd1–Pt1–Si1 52.30(8), Pd1–Pt1–Si2 54.97(8), Pt1–Pd1–Si1 56.19(8), Pt1–Pd1–Si2 54.06(8), Si1–Pt1–Si2 106.94(12), Si1–Pd1–Si2 109.91(12), Pt1–Pd1–P1 155.20 (9), Pd1–Pt1–P2 110.46(8), Pd1–Pt1–P3 133.07(9).

Chart 1



platinum complex from the reaction of silafluorene with $\text{Pt}(\eta^2\text{-C}_2\text{H}_4)(\text{PPh}_3)_2$ and assigned the structure $(\text{Ph}_3\text{P})_2\text{-Pt}(\text{H})\{\mu\text{-Si}(\text{C}_{12}\text{H}_8)\}\{\mu\text{-}\eta^2\text{-SiH}(\text{C}_{12}\text{H}_8)\}\text{Pt}(\text{PPh}_3)$ (Chart 1, B) on the basis of the NMR (^1H , ^{31}P , and ^{29}Si) spectra at -50°C .¹⁷

The ^1H NMR spectrum of **2** (25°C , 400 MHz in CD_2Cl_2) exhibits the signal for the Si–H–Pd hydrogen at δ 2.03 (Figure 3a). The $^2J(\text{PtH})$ coupling (65 Hz) is close to that of the corresponding hydrogen of $(\text{Cy}_3\text{P})\text{Pt}(\mu\text{-}\eta^2\text{-SiHPh}_2)_2\text{Pd}(\text{PCy}_3)$ (73 Hz)⁶ and smaller than that of $[(\text{Ph}_3\text{P})\text{Pt}(\mu\text{-}\eta^1, \eta^2\text{-SiH}_2\text{Ar})_2]$ (118 Hz).^{13b} The $^1J(\text{SiH})$ coupling (28 Hz) is much smaller than Si–H groups of organosilanes (190–200 Hz), which is ascribed to the Pd–H–Si three-center, two-electron bonding. The spectrum does not show a signal corresponding to the Si–H–Pt hydrogen. Although a peak at δ 1.28 is close to the Si–H–Pt hydrogen of $(\text{Cy}_3\text{P})\text{Pt}(\mu\text{-}\eta^2\text{-SiHPh}_2)_2\text{Pd}(\text{PCy}_3)$ (δ 1.70 in C_6D_6),⁶ it does not show the ^{195}Pt satellite signals at reasonable positions. The following deuterium-labeling experiment provides the unambigu-

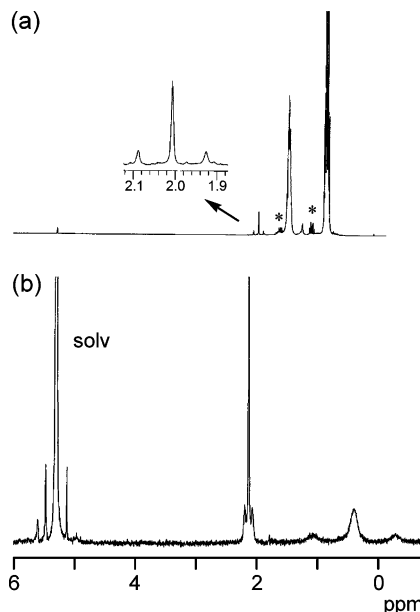


Figure 3. NMR spectra of **2** and **2-d₂**. (a) ^1H NMR of **2** at 25°C (400 MHz in CD_2Cl_2). The peaks with asterisks are attributed to contamination from the phosphine ligands in **1**. (b) ^2H NMR of **2-d₂** at 25°C (77 MHz in CH_2Cl_2).

ous evidence for the bonding mode of the hydrides and metals. The ^2H NMR spectrum of $(\text{Et}_3\text{P})_2\text{Pt}(\mu\text{-}\eta^2\text{-SiDPh}_2)_2\text{-Pd}(\text{PET}_3)$ (**2-d₂**) (25°C) contains signals at δ 2.15 ($^2J(\text{PtD}) = 10$ Hz) and 0.41 ($^1J(\text{PtD}) = 106$ Hz)¹⁸ (Figure 3b). The chemical shift and coupling constant for the latter signal support the assignment for the resonance to the deuterium in a Pt–D–Si three-center, two-electron bond. The $^1J(\text{PtH})$ value for the hydrogen bonded to Pt of **2** can be calculated to be 690 Hz by comparison of the gyromagnetic ratios of ^1H and ^2H .¹⁹ The $^{31}\text{P}\{^1\text{H}\}$ NMR spectrum at 25°C contains a single broad peak at δ 5.2, suggesting fluxional behavior of the molecule on the NMR time scale. Since the hydrides were not located in the solid state X-ray crystal structure, the exact nature of the bonding interaction is not known in the solid. The NMR data at room temperature, however, do support a M–H–Si interaction (M = Pd, Pt). Thus, complex **2** has a four-membered core composed of Pd, Pt, and two Si atoms and Pd–H–Si and Pt–H–Si bonds at room temperature in solution. Partial dissociation or intramolecular exchange of PET_3 ligands in solution is suggested by broadening of the room-temperature $^{31}\text{P}\{^1\text{H}\}$ NMR signal.¹⁵

The $^{31}\text{P}\{^1\text{H}\}$ NMR spectrum of **2** at -90°C shows a triplet and doublet ($^3J(\text{PP}) = 27$ Hz) at δ 7.2 and -0.96 . The latter signal with a large $^1J(\text{PtP})$ coupling (3223 Hz) is assigned to the phosphorus bonded to Pt. The complex contains two PET_3 ligands bonded to Pt and one PET_3 bonded to Pd center at this temperature. The ^1H NMR spectrum at -90°C gives rise to two signals for

(18) The ^2H NMR spectrum of **2-d₂** indicates the structure containing Si–D–Pd and Si–D–Pt bonding unambiguously. The ^1H NMR spectrum of **2** at 25°C , however, does not exhibit a signal around the peak position in the ^2H NMR spectrum of **2-d₂**. The ^1H NMR signal of the Pt–H–Si hydrogen may appear at δ 1.28 as a singlet or at the position that is overlapped with the PET_3 hydrogen peaks. Alternatively, serious broadening of the peak may prevent the observation of it. A large difference of the peak positions between the ^1H and ^2H NMR spectra can be accounted for by the fluxional behavior of the complex.

(19) Lide, D. R., Ed. *CRC Handbook of Chemistry and Physics*, 75th ed.; CRC Press: Boca Raton, 1994; pp 9–84. See ref 13b also.

(17) Braddock-Wilking, J.; Corey, J. C.; Dill, K.; Rath, N. P. *Organometallics* **2002**, *21*, 5467.

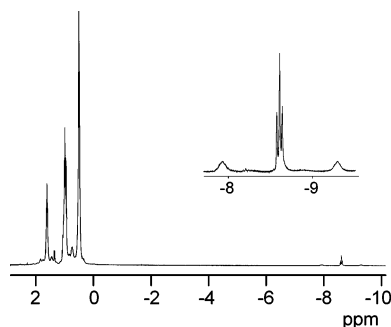
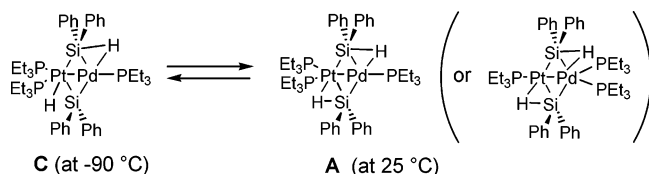
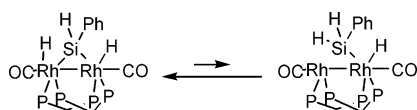


Figure 4. ^1H NMR of **2** at -90°C (400 MHz in CD_2Cl_2).

Scheme 1



Scheme 2



the PCH_2 hydrogens at δ 1.59 and 1.00 in a 1:2 signal intensity (Figure 4).

A triplet signal is observed at δ -8.61 with $^2J(\text{HP}) = 13$ Hz. It is flanked with satellite signals due to a ^{195}Pt nucleus, although the satellites by ^{29}Si are not observed. These results indicate that the signal is ascribed to a terminal hydride bonded to Pt rather than the Pt-H-Si hydrogen. Thus, complex **2** has the structure **C** in Chart 1 at -90°C in CD_2Cl_2 and the structure **A** in Chart 1 at 25°C . Change of structures occurs reversibly, as shown in Scheme 1. It involves conversion of the Pt-H bond of **C** into the Pt-H-Si bond of **A** upon raising the temperature and Si-H bond formation to regenerate **C** caused by cooling the solution. Dissociation or exchange of the phosphine ligands is suggested by the fluxional behavior of the signals. The solution at 25°C may contain a minor amount of the complex having two PEt_3 ligands at Pd and one PEt_3 at Pt also, although fluxional behavior of the complex prevents the characterization of the species by NMR. A dinuclear Rh complex with hydride and bridging SiHPh ligands was reported to be equilibrated with the complex with a terminal SiH_2Ph ligand in solution, as shown in Scheme 2.²⁰ This kind of reaction probably involves reversible conversion between the complex with hydrido and silylene ligands and an intermediate having a M-H-Si bond, as shown in Scheme 1.

The reaction of $t\text{-BuNC}$ with complex **2** at room temperature forms a mixture of $(\text{Et}_3\text{P})(t\text{-BuNC})\text{Pt}(\text{SiPh}_2\text{-CH}_2\text{-(N-}t\text{-Bu)-SiPh}_2)$ (**3**) and $(\text{Et}_3\text{P})(t\text{-BuNC})\text{Pt}(\mu\text{-SiPh}_2)_2\text{Pt}(\text{PEt}_3)(\text{CN-}t\text{-Bu})$ (**4**), as shown in eq 2. The fractional crystallization of the products leads to isolation of the complexes in respective yields of 14% and 63%. Reaction 2 gave Pd complexes with isonitrile

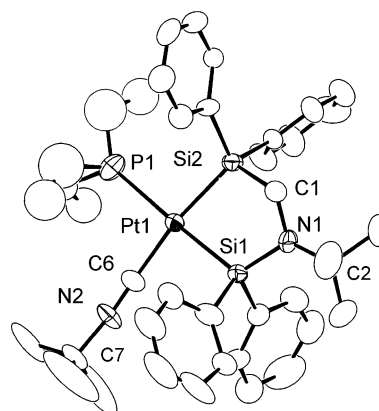
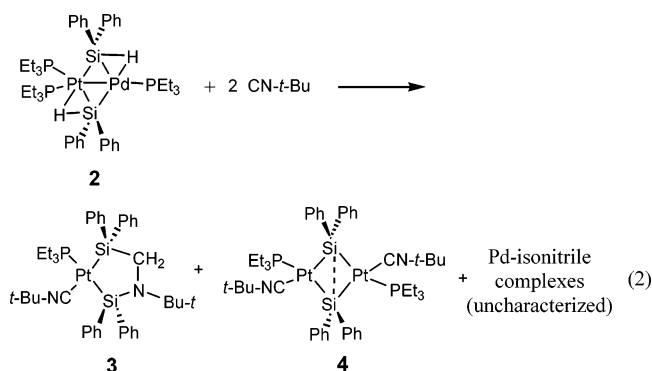


Figure 5. ORTEP drawing of **3** at the 30% ellipsoidal level. One of the two crystallographically independent molecules is shown. Selected bond distances (\AA) and angles (deg): Pt1–P1 2.392(8), Pt1–Si1 2.333(6), Pt1–Si2 2.357(5), Pt1–C6 1.97(2), Si1–N1 1.74(1), Si2–C1 1.87(2), P1–Pt1–Si1 177.4(2), P1–Pt1–Si2 96.4(3), P1–Pt1–C6 92.9(6), Si1–Pt1–Si2 81.0(2), Si1–Pt1–C6 89.7(6), Si2–Pt1–C6 170.3(6), N1–Si1–Pt1 113.0(6), C1–Si2–Pt1 106.8(6), C1–N1–Si1 113.4(9), C2–N1–Si1 125(1).

ligands, which were not isolated or characterized due to the presence of a mixture of the complexes. Figure 5 shows the molecular structure of **3** determined by X-ray crystallography.



An isomer of **3**, having the PEt_3 and isonitrile ligands at different positions from those of **3**, is not observed in the reaction mixture.

The five-membered ring in **3** is composed of Si, C, N, and Pt atoms. The carbon atom of the CH_2 group is out of the plane formed by the Pt, N, and two Si atoms. Related five-membered rings containing Pt, Si, and C have also been reported.²¹ The other product, **4**, was characterized by X-ray crystallography (Figure 6). A long Pt–Pt distance (3.9058(7) \AA) indicates a structure without a Pt–Pt bond, similar to the silylene-bridged dinuclear Pt complexes. The two Si atoms have a close contact with a separation of 2.694(6) \AA , which is slightly longer than the distance between the Si centers of the diplatinum complexes with bridging silylene ligands.^{9–11} The Pt–Si1 bond (2.385(3) \AA) is longer than the Pt–Si1* bond (2.375(4) \AA) due to a difference of the trans influence between the PEt_3 and $t\text{-BuNC}$ ligands.

Scheme 3 depicts a possible mechanism for the formation of **3**. The 1,1-insertion of isonitrile into a Pd–

(20) (a) Wang, W. D.; Eisenberg, R. *J. Am. Chem. Soc.* **1990**, *112*, 1833. (b) Wang, W. D.; Eisenberg, R. *Organometallics* **1992**, *11*, 908.

(21) Eaborn, C.; Metham, T. N.; Pidcock, A. *J. Organomet. Chem.* **1977**, *131*, 377. (b) Tanabe, M.; Yamazawa, H.; Osakada, K. *Organometallics* **2001**, *20*, 4451.

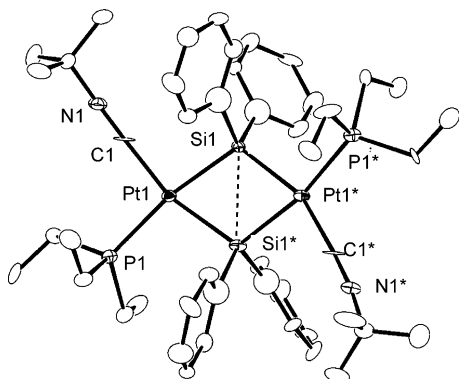
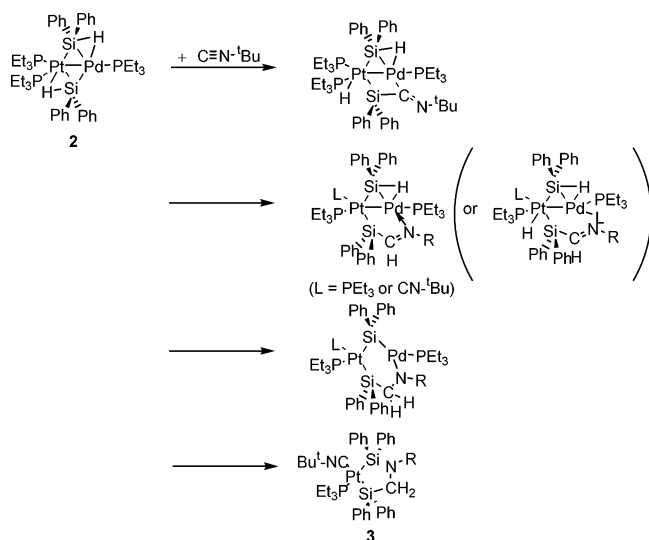


Figure 6. ORTEP drawing of **4** at the 30% ellipsoidal level. The molecule has a crystallographic C_2 symmetry center. The atoms with asterisks are crystallographically equivalent to those with the same number without asterisk. Selected bond distances (Å) and angles (deg): Pt1...Pt1* 3.9058(7), Pt1–P1 2.325(4), Pt1–Si1 2.385(3), Pt1–Si1* 2.375(4), Pt1–C1 1.97(2), Si1...Si1* 2.694(6), N1–C1 1.19(2), N1–C2 1.44(2), P1–Pt1–Si1 168.7(2), P1–Pt1–Si1* 100.3(1), P1–Pt1–C1 97.1(4), Si1–Pt1–C1 92.9(4), Si1*–Pt1–C1 159.8(4), Si1–Pt1–Si1* 68.9(1), C1–N1–C2 171(1), Pt1–C1–N1 175(1).

Scheme 3



Si bond forms a four-membered ring composed of Pt, Pd, C, and Si atoms. Subsequent transfer of the hydrogen bonded to Pt to the imine carbon leads to a Pt–Pd heterobimetallic intermediate with the iminosilyl ligand bonded to the Pt center via the Si atom. Further insertion of the C=N double bond into the Pd–H bond and reductive elimination of the aminosilane takes place. Addition of a Si–H bond in a Si ligand bonded to Fe and Pt to a CN triple bond was reported in the reaction of nitriles with the mononuclear complexes of these metals.²² Similar addition of a Si–H bond in a Ru complex to an alkene was recently reported in the mechanistic study of hydrosilylation catalyzed by Ru.²³ Reaction of acetone with a tungsten complex having a =CH(C(SiMe₃)₃) ligand also causes insertion of the C=O

bond into the Si–H bond of the complex.²⁴ The reaction in eq 2 did not give the products via insertion of isonitrile into the Pt–Si bond, while a recent study of the reaction of isonitrile with a phosphido-bridged Pt–Pt dinuclear complex revealed smooth 1,1-insertion of isonitrile into the Pt–P bond to form the product with a four-membered ring composed of P, C, and two Pt atoms.²⁵

Pathways for the formation of **4** and Pd-containing products are not clear at present, although the conversion of a silyl-Pt complex into a silylene-bridged diplatinum complex via elimination of H₂ was reported recently.^{13a} A diplatinum complex with (μ - η^2 -H-SiRH) ligands undergoes reductive elimination of H₂ upon addition of a tertiary phosphine. In reaction 2, coordination of *t*-BuNC to the Pt center induces Si–H bond activation of the diphenylsilyl ligand to produce **4**. The reaction of *t*-BuNC with **4** does not form complex **3**, indicating that **4** is not a precursor of **3** in this reaction.

The reaction of a heterodinuclear Pt–Pd complex with diphenylsilyl ligands produces the unexpected silaplatynacyclopentane containing four kinds of atoms in the five-membered ring. Detailed studies of the reactivity of late transition metal complexes toward insertion of isonitrile into the Si–H or M–Si bond are of further interest.

Experimental Section

General Methods. All manipulations of the complexes were carried out using standard Schlenk techniques under argon or nitrogen atmosphere. Hexane and toluene were distilled from sodium benzophenone ketyl and stored under nitrogen. ¹H, ²H, ¹³C{¹H}, and ³¹P{¹H} NMR spectra were recorded using JEOL GX-500, JEOL EX-400, and Varian Mercury 300 spectrometers. The peak positions in the ³¹P{¹H} NMR spectra were referenced to external 85% H₃PO₄. Pt-(SiHPh₂)₂(PEt₃)₂²⁶ and Pd(PEt₃)₃²⁷ were prepared according to the literature. *tert*-Butylisocyanide was obtained from commercial suppliers and used as received. IR absorption spectra were recorded with Shimadzu FT/IR-8100 spectrometers. Elemental analyses were carried out with a Yanaco MT-5 CHN autocorder.

Preparation of (PEt₃)Pt(μ - η^2 -HSiPh₂)₂Pd(PEt₃) (1**) and (PEt₃)₂Pt(μ - η^2 -HSiPh₂)₂Pd(PEt₃) (**2**).** A toluene (8 mL) solution containing Pd(PEt₃)₃ (290 mg, 0.70 mmol) and Pt-(SiHPh₂)₂(PEt₃)₂ (550 mg, 0.70 mmol) was stirred at room temperature for 4 h. The solvent was evaporated under reduced pressure, and the formed residue was dissolved in hexane (10 mL). Keeping the solution for 1 day at 25 °C caused separation of complex **1** as pale yellow crystals (205 mg, 34%). After removing **1** by filtration, the solvent of the filtrate was reduced to approximately 5 mL under reduced pressure and cooled at –30 °C. After 1 week, orange crystals of **2** were separated from the solution and were collected by filtration (179 mg, 25%).

Data for 1. Anal. Calcd for C₃₆H₅₂P₂PdPtSi₂: C, 47.81; H, 5.80. Found: C, 47.68; H, 5.53. ¹H NMR (400 MHz, C₆D₆, 25 °C): δ 8.20 (d, 1H, C₆H₅-*o*, *J*(HH) = 8 Hz), 8.08 (d, 3H, C₆H₅-*o*, *J*(HH) = 8 Hz), 8.06 (d, 3H, C₆H₅-*o*, *J*(HH) = 8 Hz), 8.01 (d, 1H, C₆H₅-*o*, *J*(HH) = 8 Hz), 7.32 (t, 4H, C₆H₅-*m*, *J*(HH) = 8 Hz), 7.28 (t, 4H, C₆H₅-*m*, *J*(HH) = 7 Hz), 7.18 (t, 4H, C₆H₅-*p*,

(24) Watanabe, T.; Hashimoto, H.; Tobita, H. *Angew. Chem., Int. Ed.* **2004**, *43*, 218.

(25) Cristofani, S.; Leoni, P.; Pasquali, M.; Eisentraeger, F.; Albinati, A. *Organometallics* **2000**, *19*, 4589.

(26) Kim, Y.-J.; Park, J.-I.; Lee, S.-C.; Osakada, K.; Tanabe, M.; Choi, J.-C.; Koizumi, T.; Yamamoto, T. *Organometallics* **1999**, *18*, 1349.

(27) Schunn, R. A. *Inorg. Chem.* **1976**, *15*, 208.

(22) (a) Corriu, R. J. P.; Moreau, J. J. E.; Pataud-Sat, M. *Organometallics* **1985**, *4*, 623. (b) Tanabe, M.; Osakada, K. *Organometallics* **2001**, *20*, 2118. See also: Murai, T.; Sakane, T.; Kato, S. *Tetrahedron Lett.* **1985**, *26*, 5145.

(23) Glaser, P. B.; Tilley, T. D. *J. Am. Chem. Soc.* **2003**, *125*, 13640.

Table 1. Crystallographic Data and Details of Refinement

	1	2	3	4
chemical formula	C ₃₆ H ₅₀ P ₂ PdPtSi ₂	C ₄₂ H ₆₅ P ₃ PdPtSi ₂	C ₄₀ H ₅₅ N ₂ P ₂ PtSi ₂	C ₄₆ H ₆₈ N ₂ Si ₂ P ₂ Pt ₂
fw	902.40	1020.56	846.12	1157.36
cryst syst	triclinic	triclinic	triclinic	monoclinic
space group	<i>P</i> $\bar{1}$ (No. 2)	<i>P</i> $\bar{1}$ (No. 2)	<i>P</i> $\bar{1}$ (No. 1)	<i>C</i> 2/ <i>c</i> (No. 15)
<i>a</i> , Å	9.6294(7)	11.8945(5)	11.787(3)	19.222(5)
<i>b</i> , Å	10.1484(5)	20.3726(8)	12.124(3)	11.727(2)
<i>c</i> , Å	11.3224(1)	21.3757(7)	17.936(6)	22.376(5)
α , deg		78.89(3)	73.20(2)	
β , deg	68.03(3)	73.11(2)	81.52(2)	106.47(1)
γ , deg	64.21(2)	78.03(2)	58.98(1)	
<i>V</i> , Å ³	923.27(8)	4494.1(3)	2102.8(10)	4836.7(20)
<i>Z</i>	1	4	2	4
μ , mm ⁻¹	4.431	3.684	3.445	5.902
<i>F</i> (000)	450	2056	860	2288
<i>D</i> _{calcd} , g cm ⁻³	1.627	1.508	1.336	1.589
cryst size, mm × mm × mm	0.50 × 0.50 × 0.50	0.55 × 0.32 × 0.25	0.30 × 0.15 × 0.10	0.20 × 0.15 × 0.10
no. of unique reflns	5206	18 826	8664	5445
no. of reflns used (<i>I</i> > 3.0σ(<i>I</i>))	5075	13 764	6656	3397
no. of variables	215	1021	859	278
<i>R</i>	0.044	0.066	0.043	0.044
<i>R</i> _w	0.071	0.081	0.053	0.073
GOF	1.13	2.17	0.989	0.096

J(HH) = 8 Hz), 2.71 (d, 1H, Pd-*H*-Si, ²*J*(HPt) = 96 Hz, ²*J*(HP) = 13 Hz), 2.06 (d, 1H, Pt-*H*-Si, ¹*J*(HPt) = 650 Hz, ²*J*(HP) = 13 Hz), 1.49 (m, 6H, PCH₂), 1.27 (apparent quintet due to virtual coupling, 6H, PCH₂), 0.71 (m, 18H, PCH₂CH₃). ¹³C{¹H} NMR (100 MHz, CD₂Cl₂, 25 °C): δ 147.1 (s, C₆H₅-*l*), 144.7 (s, C₆H₅-*l*), 136.4 (s, C₆H₅-*o*), 136.1 (s, C₆H₅-*o*), 128.5 (s, C₆H₅-*m*), 128.1 (s, C₆H₅-*p*), 127.6 (s, C₆H₅-*m*), 22.2 (d, PCH₂, ¹*J*(CP) = 29 Hz), 20.8 (d, PCH₂, ¹*J*(CP) = 20 Hz), 9.0 (s, CH₃), 8.9 (s, CH₃). ³¹P{¹H} NMR (162 MHz, CD₂Cl₂, 25 °C): δ 28.3 (d, Pt-*P*, ¹*J*(PPt) = 3556 Hz, ³*J*(PP) = 55 Hz), 15.8 (d, Pd-*P*, ²*J*(PPt) = 258 Hz, ³*J*(PP) = 55 Hz).

Data for 2. Anal. Calcd for C₄₂H₆₇P₃PdPtSi₂: C, 49.33; H, 6.60. Found: C, 49.73; H, 6.07. ¹H NMR (400 MHz, CD₂Cl₂, 25 °C): δ 7.70 (d, 4H, C₆H₅-*o*), 7.68 (d, 4H, C₆H₅-*o*, *J*(HH) = 6 Hz), 7.31 (t, 4H, C₆H₅-*m*, *J*(HH) = 6 Hz), 7.28 (t, 4H, C₆H₅-*m*, *J*(HH) = 6 Hz), 7.26 (t, 4H, C₆H₅-*p*, *J*(HH) = 6 Hz), 2.03 (s, 1H, Pd-*H*-Si, ²*J*(HPt) = 65 Hz, ¹*J*(HSi) = 28 Hz), 1.28 (s, 1H, see Results and Discussion), 1.50 (br, 18H, PCH₂), 0.87 (br, 27H, CH₃). ¹H NMR (400 MHz, CD₂Cl₂, -90 °C): δ 7.54 (br, 8H, C₆H₅-*o*), 7.20 (br, 8H, C₆H₅-*m*, *J*(HH) = 5 Hz), 7.14 (br, 4H, C₆H₅-*p*), 1.59 (br, 6H, PCH₂), 1.00 (m, 12H, PCH₂), 0.48 (br, 27H, CH₃), -8.61 (t, 1H, Pt-*H*, ¹*J*(HPt) = 550 Hz, ²*J*(HP) = 13 Hz). ¹³C{¹H} NMR (100 MHz, CD₂Cl₂, -90 °C): δ 150.8 (s, C₆H₅-*l*), 146.6 (s, C₆H₅-*l*), 134.6 (s, C₆H₅-*o*), 126.7 (s, C₆H₅-*p*), 126.5 (s, C₆H₅-*m*), 126.0 (s, C₆H₅-*m*), 20.9 (br, Pt-PCH₂), 19.2 (d, Pd-PCH₂), 8.3 (s, Pd-PCH₂CH₃), 7.9 (s, Pt-PCH₂CH₃). ³¹P{¹H} NMR (162 MHz, CD₂Cl₂, 25 °C): δ 5.2 (br). ³¹P{¹H} NMR (162 MHz, CD₂Cl₂, -90 °C): δ 7.2 (t, Pd-*P*, ²*J*(PPt) = 243 Hz, ³*J*(PP) = 27 Hz), -0.96 (d, Pt-*P*, ¹*J*(PPt) = 3223 Hz, ³*J*(PP) = 27 Hz).

Preparation of (PEt₃)Pt(μ-η²-DSiPh₂)₂Pd(PEt₃) (1-d₂) and (PEt₃)₂Pt(μ-η²-DSiPh₂)₂Pd(PEt₃) (2-d₂). These complexes were prepared by using D₂SiPh₂ analogously. ²H NMR of 1-d₂ (77 MHz, C₆H₆-C₆D₆, 25 °C): δ 2.74 (s, Pd-*D*-Si, ²*J*(DPt) = 15 Hz), 2.07 (s, Pt-*D*-Si, ¹*J*(DPt) = 90 Hz). ²H NMR of 2-d₂ (77 MHz, C₆H₆-C₆D₆, 25 °C): δ 2.51 (s, Pd-*D*-Si, ²*J*(DPt) = 11 Hz), -0.29 (br, Pt-*D*-Si, ¹*J*(DPt) = 96 Hz); (77 MHz, CH₂-Cl₂-CD₂Cl₂, 25 °C): δ 2.15 (s, Pd-*D*-Si, ²*J*(DPt) = 10 Hz), 0.41 (br, Pt-*D*-Si, ¹*J*(DPt) = 106 Hz).

Preparation of Pt(SiPh₂-CH₂-NC(CH₃)₃-SiPh₂)(CNC-(CH₃)₃)(PEt₃) (3) and [(Et₃P)Pt(μ-SiPh₂)(CNC(CH₃)₃)]₂ (4). To a hexane (5 mL) solution of 2 (250 mg, 0.24 mmol) was added *tert*-butylisocyanide (58 μL, 0.51 mmol) at room temperature. After stirring the reaction mixture for 4 h a yellow solid was precipitated. The solid was collected by filtration, washed with hexane (2 mL), and dried in vacuo to give 4 (90

mg, 63%). The combined filtrate and washings were stored for 3 days at -30 °C to form a white solid, which was collected by filtration to give 3 (15 mg, 14%). Data for 3: Anal. Calcd for C₄₀H₅₅N₂P₂PtSi₂: C, 56.78; H, 6.55; N, 3.31. Found: C, 56.35; H, 6.34; N, 2.88. ¹H NMR (400 MHz, C₆D₆, rt): δ 8.10 (d, 4H, C₆H₅-*o*, *J*(HH) = 8 Hz), 7.96 (d, 4H, C₆H₅-*o*, *J*(HH) = 8 Hz), 7.33 (t, 4H, C₆H₅-*m*, *J*(HH) = 8 Hz), 7.32 (t, 4H, C₆H₅-*m*, *J*(HH) = 8 Hz), 7.24 (t, 2H, C₆H₅-*p*, *J*(HH) = 8 Hz), 7.18 (t, 2H, C₆H₅-*p*, *J*(HH) = 8 Hz), 3.55 (s, 2H, CH₂, ³*J*(HPt) = 41 Hz), 1.24 (s, 9H, Si-NC(CH₃)₃), 1.22 (m, 6H, PCH₂CH₃), 0.76 (s, 9H, Pt-CNC(CH₃)₃), 0.64 (m, 9H, PCH₂CH₃). ¹³C{¹H} NMR (126 MHz, C₆D₆, rt): δ 149.9 (s, C₆H₅-*l*), 145.9 (s, C₆H₅-*l*), 137.3 (s, C₆H₅-*o*, ²*J*(Cpt) = 15 Hz), 136.2 (s, C₆H₅-*o*, ²*J*(Cpt) = 15 Hz), 127.3 (s, C₆H₅-*m*), 126.9 (s, C₆H₅-*m*), 56.4 (s, C(CH₃)₃), 54.4 (s, C(CH₃)₃, ³*J*(Cpt) = 22 Hz), 45.7 (d, CH₂, ³*J*(CP) = 8 Hz, ²*J*(Cpt) = 107 Hz), 30.7 (s, C(CH₃)₃), 29.4 (s, C(CH₃)₃), 18.7 (d, PCH₂, ²*J*(CP) = 22 Hz, ³*J*(Cpt) = 42 Hz), 8.6 (s, PCH₂CH₃, ³*J*(Cpt) = 18 Hz). The signals of C₆H₅-*p* are overlapped with solvent signals. ³¹P{¹H} NMR (162 MHz, C₆D₆, rt): δ 18.1 (s, ¹*J*(PPt) = 1545 Hz). IR (KBr, cm⁻¹): 2157 ν(CN).

Data for 4. Anal. Calcd for C₄₆H₆₈N₂P₂Pt₂Si₂: C, 47.74; H, 5.92; N, 2.42. Found: C, 47.89; H, 5.98; N, 2.43. ¹H NMR (400 MHz, C₆D₆, rt): δ 8.16 (d, 8H, C₆H₅-*o*), 7.27 (t, 8H, C₆H₅-*m*), 7.12 (t, 4H, C₆H₅-*p*), 1.38 (dq, 12H, PCH₂CH₃, ²*J*(HP) = 8 Hz), 0.91 (s, 18H, C(CH₃)₃), 0.88 (dt, 18H, PCH₂CH₃, ³*J*(HP) = 8 Hz). ¹³C{¹H} NMR (100 MHz, C₆D₆, rt): δ 152.5 (s, C₆H₅-*l*), 137.9 (s, C₆H₅-*o*, ³*J*(Cpt) = 26 Hz), 126.2 (s, C₆H₅-*m*), 125.7 (s, C₆H₅-*p*), 55.6 (s, C(CH₃)₃), 29.8 (s, C(CH₃)₃), 19.7 (m, PCH₂-CH₃, ²*J*(Cpt) = 36 Hz), 8.89 (s, PCH₂CH₃, ³*J*(Cpt) = 16 Hz). ³¹P{¹H} NMR (162 MHz, C₆D₆, rt): δ 24.4 (s, ¹*J*(PPt) = 1495 Hz, ³*J*(PPt) = 245 Hz, ⁴*J*(PP) = 32 Hz). IR (KBr, cm⁻¹): 2132 ν(CN).

X-ray Crystallography. Crystals of 1–4 suitable for X-ray diffraction studies were mounted in glass capillaries under argon. Data were collected at -180 °C on a Rigaku Saturn CCD area detector equipped with graphite-monochromated Mo Kα radiation (λ = 0.71073 Å). A total of 720 oscillation images were collected. A sweep of data was done using ω scans from -110.0° to 70.0° in 0.5° step, at χ = 45.0° and φ = 0.0°. The detector swing angle was -20.32°. The crystal-to-detector distance was 45.00 mm. Readout was performed in the 0.070 mm pixel mode. Calculations were carried out by using the program package Crystal Structure for Windows. The structure was solved by direct methods and expanded using Fourier techniques. A full-matrix least-squares refinement was used for the non-hydrogen atoms with anisotropic thermal param-

eters. Crystallographic data and details of structure refinement are summarized in Table 1.

Acknowledgment. This work was supported by a Grant-in-Aid for Scientific Research from the Ministry of Education, Science, Sports, and Culture, Japan.

Supporting Information Available: Crystallographic data of **1–4**. This material is available free of charge via the Internet at <http://pubs.acs.org>.

OM049858D